This is a repository copy of *Ba(OH)(2) - blast furnace slag composite binders for encapsulation of sulphate bearing nuclear waste*.

Article:

Ba(OH)$_2$– blast furnace slag composite binders for the encapsulation of sulphate bearing nuclear waste

Neda Mobasher[1], Hajime Kinoshita[1], Susan A. Bernal[1], Clint A. Sharrard[2]

[1]Immobolisation Science Laboratory, Department of Materials Science & Engineering, The University of Sheffield, Sheffield S1 3JD, United Kingdom

[2] Centre for Radiochemistry Research, School of Chemistry, The University of Manchester, Oxford Road, Manchester M13 9PL, United Kingdom

Abstract

The present study investigated the feasibility of the immobilisation of sulphate bearing radioactive wastes in blast furnace slag (BFS)-based binders. BaSO$_4$-BFS composites were produced via two methods using Na$_2$SO$_4$ as a waste simulant, along with Ba(OH)$_2$ to promote precipitation of BaSO$_4$ in an insoluble sulphate form and the consequent activation of the BFS. BaSO$_4$ was effectively formed by both methods, and solid wasteforms were successfully produced. Although both methods produced BaSO$_4$ embedded in the cement-like composites, different reaction products including ettringite and witherite were produced, depending on the order Ba(OH)$_2$ was mixed with the system. These results show that the immobilisation of soluble sulphate-bearing aqueous wastes is achievable in Na$_2$SO$_4$-Ba(OH)$_2$-BFS composites.

Keywords: barium hydroxide, alkali-activated slag, sodium sulphate, nuclear wastes

1. Introduction

One of the most important challenges facing the global nuclear industry is the safe and secure disposal of radioactive wastes. Various technologies have been adopted for the encapsulation and immobilisation of radioactive waste, and the most successful examples are vitrification[1] and encapsulation in Portland cement-based materials (also known as cementation).[2] However, the encapsulation of sulphate bearing radioactive waste e.g., ion exchange resins in the UK nuclear waste stream[3] is difficult to achieve via vitrification in borosilicate matrices

due to its low solubility, which leads to the formation of secondary phases and the swelling of the vitreous mass.[4] In the case of cementation with Portland cement, the excess of dissolved sulphate ions promotes microstructural changes, i.e the transformation of calcium monosulphoaluminate (AFm phase, $Ca_4Al_2(OH)_{12}(SO_4).6H_2O$) to ettringite ($Ca_6Al_2(OH)_{12}(SO_4)_3.26H_2O$) whose large molar volume causes expansion and cracking, resulting in the potential release of radionuclides into the environment.[5-7]

Alkali-activated binders are materials produced through the chemical reaction between an aluminosilicate source and an alkali activator that develop high mechanical strength, along with reduced permeability, at early times of curing. In recent years it has been suggested that alkaline activated slag (AAS) might be a better option for stabilisation/solidification of low/intermediate level waste (LLW/ILW) than Portland cement due to its low permeability, low reaction heat, and high resistance to aggressive chemical attack [8-10]. The activation of slag using near-neutral salts such as Na_2CO_3 and Na_2SO_4 has been considered a potential alternative for the immobilisation of nuclear wastes including reactive metals.[11] The other utilisation of these binders in the area of radioactive waste treatment includes the solidification of spent ion exchange resins,[12] and stabilisation/ solidification (S/S) treatment of radioisotopes including ^{152}Eu, ^{60}Co and ^{59}Fe,[13] ^{99}Tc,[14, 15] and ^{129}I.[15] This elucidates that these alternative cements have the potential to play an important role in the current and future radioactive waste clean-up.

Asano et al.[16] recently reported a possible S/S process for sulphate-rich aqueous LLW using $Ba(OH)_2$ and BFS via a two-step process in which a cement-like solid can be formed. In the first step, Na_2SO_4 (simulated waste) solution was mixed with $Ba(OH)_2$, stabilising the sulphate ions through the precipitation of $BaSO_4$ and forming cement-like solids in the second step. Composite cement-like systems of this type would be beneficial not only for the formation of very low-solubility $BaSO_4$ ($Ksp \approx 10^{-10}$ mol^2/L^2), but may also be valuable because $BaSO_4$ can enhance the radiation shielding properties of concrete due to the high atomic number of Ba.[18]

The aim of the present study is the synthesis and characterisation of $BaSO_4$-BFS composite cement-like systems for immobilisation of sulphate-bearing nuclear wastes via two methods. A two-step process based on the work of Asano et al.[16] was further studied, with initial mixing of sulphate-containing waste stimulant (Na_2SO_4) and $Ba(OH)_2$ and later blending with

BFS ("method A"). An alternative one-step process ("method B") was also tested, where the Na_2SO_4 and $Ba(OH)_2$ are blended directly with BFS promoting the simultaneous formation of $BaSO_4$ and the binding phases derived from the alkali-activation of the BFS. The reaction products formed from both methods are studied using X-ray diffraction (XRD), thermogravimetry and scanning electron microscopy, to assess the feasibility of these methods.

2. Materials and methods

2.1. Materials

A BFS from Redcar steel works with a specific surface of 286 m^2/kg was used as the main binding precursor, whose chemical composition is presented in Table 1. Barium hydroxide octa-hydrate ($Ba(OH)_2 \cdot 8H_2O$, 97% purity), and sodium sulphate (Na_2SO_4, 99% purity) from Alfa Aesar were used for producing the composites.

Table 1. Composition of blast furnace slag, from X-ray fluorescence analysis. LOI is loss on ignition at 1000°C

Component (mass % as oxides)	CaO	SiO_2	Al_2O_3	Fe_2O_3	MgO	K_2O	Na_2O	Others	LOI	Total
BFS	42.1	34.5	13.7	0.97	7.29	0.49	0.22	0.69	-1.05	98.9

2.2. Mixing procedures

Method A - A simulated aqueous sulphate waste was prepared by dissolving 10 wt.% Na_2SO_4 in distilled water at 40°C. $Ba(OH)_2 \cdot 8H_2O$ was weighed and added to the simulated sulphate waste with a molar ratio of Ba/SO_4 of 1.3:1, and mixed for 3 hours at 60°C. The obtained slurry was added to BFS at water to binder (w/b) ratio of 0.35 and placed in a sealed plastic centrifugal tube. The samples were manually shaken for 2 to 5 minutes at room temperature and then further mixed for 5 minutes using a Whirh Mixer. This formulation was identified as optimal by Asano et al.[16] who achieved a 98% conversion of Na_2SO_4 to the $BaSO_4$, and it is used in this study as a reference to evaluate the effectiveness of method B.

Method B – A simulated aqueous sulphate waste prepared with the same procedure used in Method A was mixed with an homogenous blend of unreacted BFS and powdered $Ba(OH)_2 \cdot 8H_2O$. The samples were manually shaken for 2 to 5 minutes in a sealed centrifuge tube at room temperature, then further mixed for 5 minutes using a Whirh Mixer. Detailed formulations of the specimens produced are given in Table 2.

Table 2. Formulations of Na_2SO_4-$Ba(OH)_2$-BFS composites produced via method B

Sample ID	BFS (g)	$Ba(OH)_2 \cdot 8H_2O$ (g)	H_2O (g)	Ba^{2+}/SO_4^{2-} molar ratio	water/binder ratio
M0	100	0	35	0 : 1	0.35
M1	100	8.64	35	1.0 : 1	0.35
M1.1	100	9.51	35	1.1 : 1	0.35
M1.2	100	10.37	35	1.2 : 1	0.35
M1.3	100	11.23	35	1.3 : 1	0.35

Hardened specimens stored for 33 days at room temperature were de-moulded, crushed and immersed in acetone to arrest the reaction process. After several days, the samples were removed from the acetone, air dried and desiccated under vacuum. The dried samples were kept in sealed containers prior to analysis to avoid carbonation. The phase analysis of the products was conducted by XRD using a Siemens D500 X-ray diffractometer with monochromatic Cu Kα radiation (λ=1.5405 Å), operated at a step size of 0.02° and scanning speed of 2°/min between 5° and 65° 2θ. The samples were also subjected to thermogravimetric analysis using a Perkin Elmer Pyris 1 TGA. Approximately 40 mg of powdered samples were weighed, placed and heated in an alumina crucible under flowing nitrogen. A constant heating rate of 10°C/min was used from room temperature up to 1000°C. Microstructural characterisation was performed by Scanning Electron Microscopy (SEM) using a JEOL JSM 6400 electron microscope with a 20 kV accelerating voltage and a working distance of 10 mm. Carbon coated polished samples were evaluated using backscattered electron mode. A Link-Isis (Oxford Instruments) X-ray energy dispersive (EDX) detector was used for the elemental analysis.

3. Results and discussion

3.1. Method A

The X-ray diffractograms of the anhydrous BFS (Figure 1) show peaks attributed to gehlenite ($Ca_2Al_2SiO_7$) and calcite ($CaCO_3$). In addition to these phases, calcium silicate hydrate (C-S-H) and hydrotalcite ($Mg_3[Al(OH)_8](CO_3)_{0.5}$) were identified in the product from Method A. High-intensity peaks for $BaSO_4$ are also observed, confirming the formation of this salt in the two step procedure.
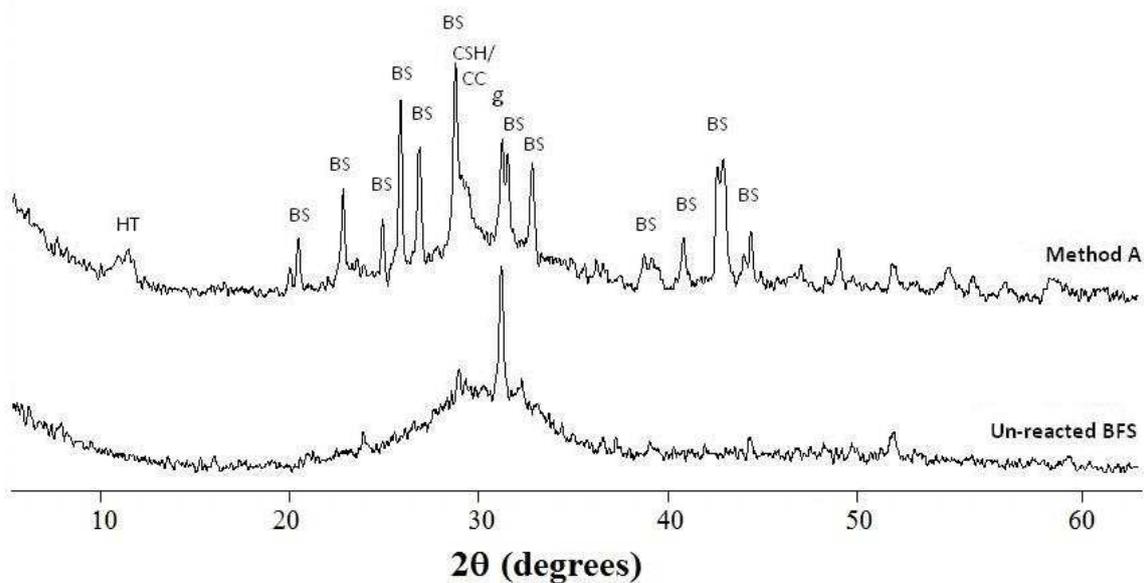
Fig. 1. X-ray diffractograms of the unreacted slag, and the sulphate-BFS composite produced via Method A. Peaks marked are $BaSO_4$ (BS), gehlenite (g: $Ca_2Al_2SiO_7$), hydrotalcite (HT: $Mg_3[Al(OH)_8](CO_3)_{0.5}$), calcite (CC: $CaCO_3$) and calcium silicate hydrate (C-S-H)

Thermogravimetry results for this specimen (not shown) indicated a total mass loss of 11%, including a significant mass loss (~7%) between 25°C and 400°C, associated with the dehydration of the C-S-H and hydrotalcite[18], and 4% mass loss between 550°C and 680°C assigned to the decomposition of the calcite both of which confirms the XRD results. The formation of C-S-H and hydrotalcite in the BFS system have been reported from NaOH activation[18]. Therefore, the obtained result suggests that in method A, NaOH was produced as a secondary product during the formation of $BaSO_4$ in the first step as shown in Eq. 1, and acted as an alkaline activator to promote the hardening of the $BaSO_4$-BFS composite.

$$Na_2SO_4 + Ba(OH)_2 \longrightarrow BaSO_4 + 2NaOH \qquad (1)$$

In the backscattered electron image of the specimens produced via method A (Fig. 2), un-reacted BFS is identified as light grey angular particles, corresponding to the areas enriched in Ca and Si in the elemental maps. The small white particles intermixed with the binding phase are confirmed to be $BaSO_4$ by the distribution of Ba and S in the elemental map.
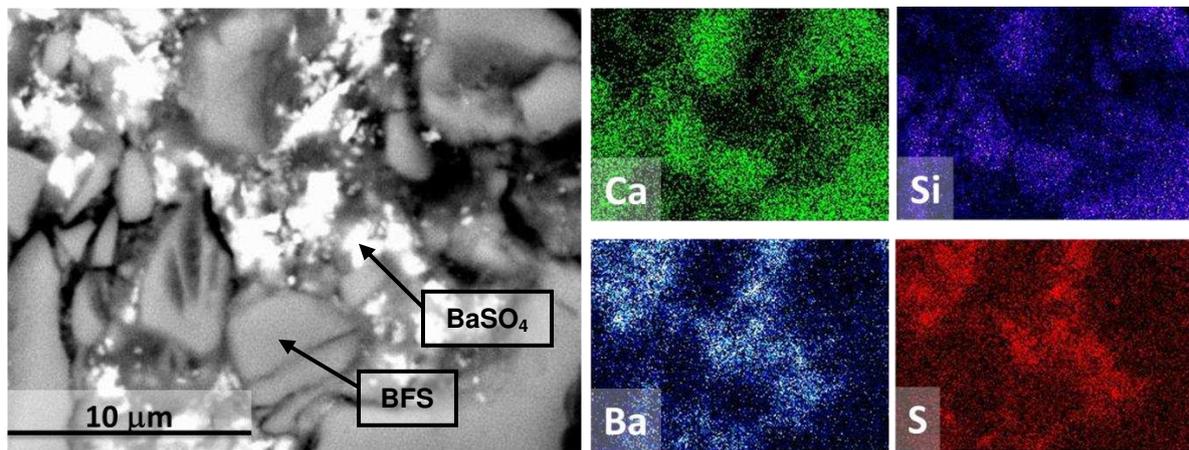
Fig. 2. Backscattered electron image and elemental maps of sulphate-BFS composite cement produced via method A. The elemental maps show the same region as the backscattered electron image.

3.2. Method B

The XRD patterns of the samples produced via this method (Fig. 3) again showed gehlenite and calcite from the unreacted slag. As main crystalline products, $BaSO_4$, ettringite, portlandite $(Ca(OH)_2)$ and witherite $(BaCO_3)$ were observed in addition to C-S-H. The formation of ettringite was clear in the sample without $Ba(OH)_2$ (Figure 3, sample M0), due to the high concentration of sulphates in the system. In samples including $Ba(OH)_2$ (Samples M1.1, M1.2 and M1.3), formation of $BaSO_4$ was observed. The intensities of the $BaSO_4$ and C-S-H peaks appeared to increase with higher contents of $Ba(OH)_2$, suggesting that the addition of $Ba(OH)_2$ promotes a higher extent of $BaSO_4$ formation as well as higher BFS dissolution, as it is likely contributing to increase the alkalinity of the system.

Reduction in the intensity of the ettringite peaks was also observed with increasing $Ba(OH)_2$ addition and the higher alkalinity provided to the system, consistent with the increased $BaSO_4$ formation. Witherite peaks were also observed in the binders including $Ba(OH)_2$, whose

intensity increases with a higher content of Ba^{2+} in the system, along with the formation of higher intensity peaks of portlandite. This may suggest that $Ba(OH)_2$ is reacting with the $CaCO_3$ present in the system as shown in Eq. 2:

$$Ba(OH)_2 + CaCO_3 \longrightarrow BaCO_3 + Ca(OH)_2 \quad (2)$$

This reaction is thermodynamically favourable ($\Delta G = -51.66$ kJ/mol) at 25°C. The formation of $BaCO_3$ might also be indicating the preferential carbonation of Ba^{2+} in the pore solution instead of carbonation of Na^+ or Ca^{2+}, driving the system towards the formation of $BaCO_3$.
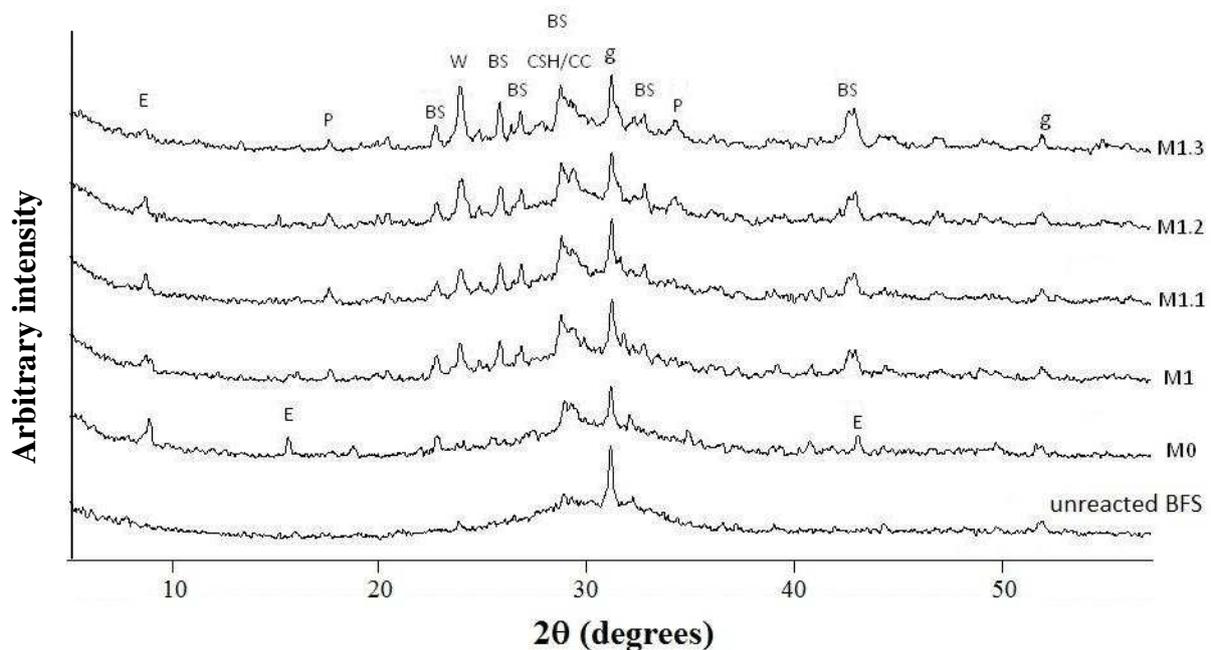
Fig. 3. X-ray diffractograms of sulphate-BFS composite produced via the method B, as a function of the sulphate:$Ba(OH)_2$ ratio. Peaks marked are $BaSO_4$ (BS), gehlenite (g: $Ca_2Al_2SiO_7$), calcite (CC: $CaCO_3$), calcium silicate hydrate (C-S-H), portlandite (P: $Ca(OH)_2$), witherite (W: $BaCO_3$) and ettringite (E: $Ca_6Al_2(OH)_{12}(SO_4)_3.26H_2O$).

Fig. 4 shows the derivative thermograms (DTG) of the composite binders. The total mass loss for these samples varies between 10% and 11%, independently of the $Ba^{2+}:SO_4^{2-}$ molar ratio. In the specimen without $Ba(OH)_2$ (M0), a high intensity peak between 70°C and 200°C was observed, which is attributed to the release of evaporable water in the system, and the starting dehydration of the monosulphoaluminate [19] and ettringite [20] identified through XRD. The progressive mass loss between 200°C and 400°C is assigned to the decomposition of the C-S-

H forming in this specimen also identified through XRD. The low intensity shoulder around 550°C is attributed to the decomposition of calcite [21].
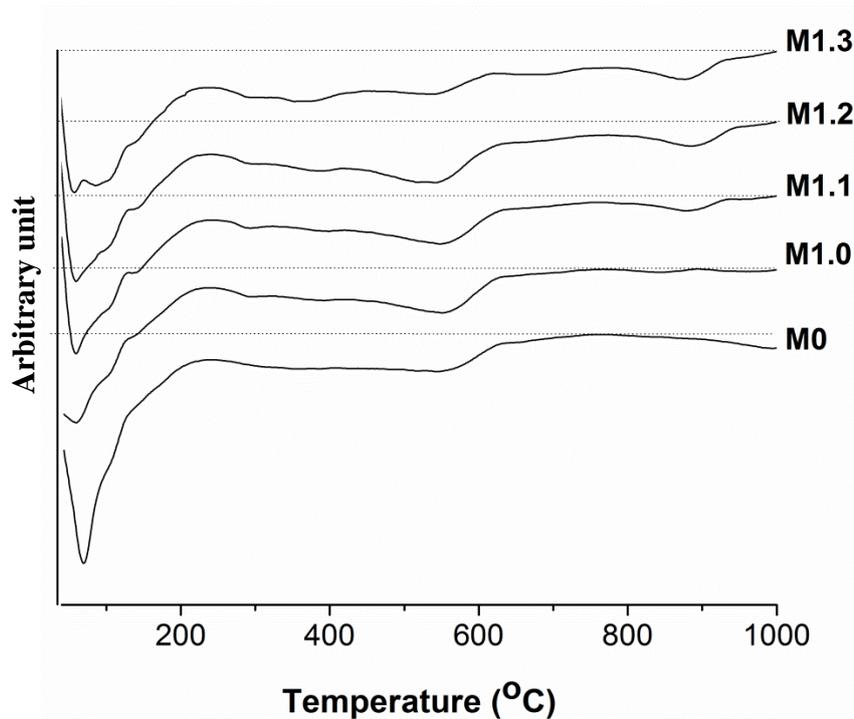
Fig. 4. Derivative thermograms (mass loss downwards) of $BaSO_4$-BFS composites as a function of the $Ba(OH)_2$:Na_2SO_4 ratio in the system. Dashed lines show the baseline for each data set.

Samples including lower concentrations of $Ba(OH)_2$ (Fig. 4., sample M1.0) showed a significant broadening and a reduced intensity of the first part of mass loss between 70°C and 200°C when compared with the specimen without $Ba(OH)_2$ (M0), possibility of less ettringite formation in the system. In this case the peaks identified approximately at 80°C to 100°C correspond to the release of evaporable water and the dehydration of the mono-sulphoaluminates and ettringite as discussed above. An increased mass loss from 100°C up to 250°C could be assigned to the dehydration of water from small pores in C-S-H, or potentially from disordered hydrotalcite or AFm type phases,[22] as these are often observed in slag-containing binders. The amount of these phases could be small as they were not observed in the XRD results, it is also possible that the inclusion of Ba in these systems induces modification of the structure of these types of products via a cation exchange

mechanism between Ba^{2+} and Ca^{2+} or Mg^{2+} (comparable to the mechanisms identified in zeolites [23]), making the phases disordered and rendering identification through XRD difficult.

In sulphate-activated binders traces of mirabilite ($Na_2SO_4 \cdot 10H_2O$) is often identified [24], which forms as a result of excess of Na_2SO_4 in the system and precipitates from the pore solution during the drying of the samples. Considering the high content of dissolved sulphates included in the method B binders, traces of mirabilite can be expected at the lower $Ba(OH)_2$ concentrations, although it was not identified by XRD. Based on this, part of the intensity of the first mass loss could be assigned to the dehydration of mirabilite, which occurs at 40°C. The progressive mass loss between 250°C and 400°C is again assigned to the thermal decomposition of highly crosslinked C-S-H forming in this binder, which seems to have water more tightly bound than C-S-H formed in the specimen formulated without $Ba(OH)_2$. The shoulder assigned to calcite decomposition seems to become more distinct in the specimens M1.0, M1.1 and M1.2 than in the sample without $Ba(OH)_2$ (M0), indicating an extended carbonation of the M1.0, M1.1 and M1.2 samples, which could be consequence of the increased alkalinity in the system associated with the inclusion of $Ba(OH)_2$.

A similar trend was identified in specimens with increased $Ba(OH)_2$ (Fig. 4. samples M1.1, M1.2 and M1.3), where reductions in the intensity of the peak around 80°C with increasing addition of $Ba(OH)_2$ are observed, consistent with an extended reaction between the Na_2SO_4 and the $Ba(OH)_2$ towards the formation of $BaSO_4$, and a possible reduction of ettringite as identified by XRD. A more defined and higher intensity shoulder was observed between 100°C and 250°C, indicating the formation of a larger amount of reaction products in these composites with the increment of $Ba(OH)_2$, as a rise of alkalinity favoured the dissolution of the BFS. In specimens formulated with higher $Ba(OH)_2$ concentrations, a peak at 800°C was observed, which was due to the decomposition of either the small quantity of excess $Ba(OH)_2$ or $BaCO_3$ present. Increased intensity of this peak was observed with higher Ba^{2+} in the system, along with reduced intensities of the mass loss assigned to decomposition of calcite, consistent with Eq. 1.

Fine white particles intermixed in the binding matrix of activated BFS were identified in the composites produced via method B (Fig. 5), consistent with that identified in the specimens produced via method A (Fig. 2). However in contrast to the observations for the specimen

produced via method A (Fig. 2), BaSO$_4$ clusters were not identified in this specimen, which might suggest a better intermixing and distribution of the BaSO$_4$ particles.
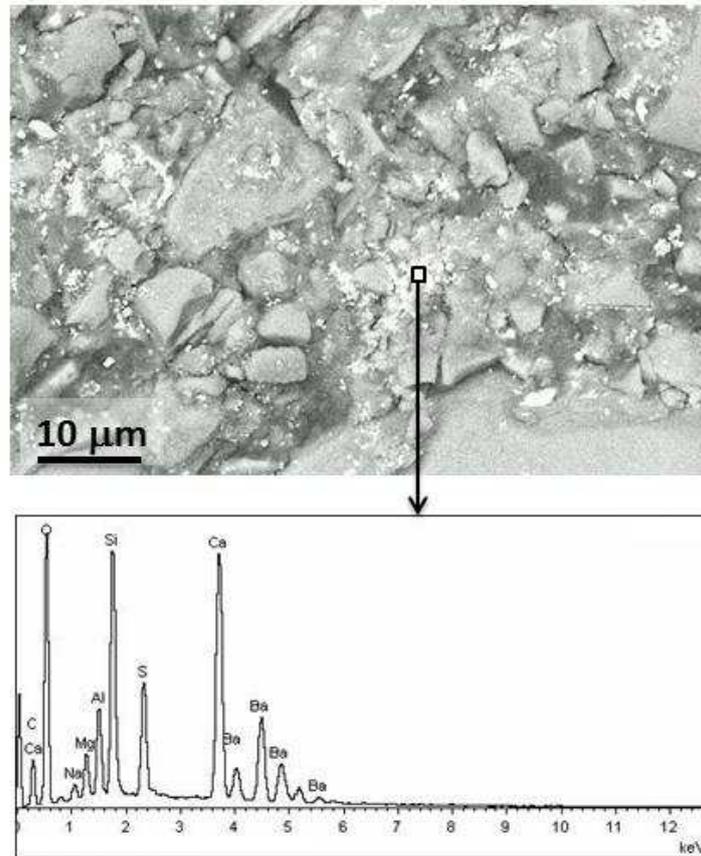
Fig. 5. Backscattered electron image and EDX spectra of sulphate-BFS composite (M1.2) produced via method B

In terms of immobilisation of sulphate ions, method A thus allows a better control, and closer approach to completion of the reaction to convert all of the sulphate ions into BaSO$_4$, with a minor excess of Ba^{2+} within the system; although, lower extents of reaction of BFS could be expected in these binders when compared with the one-step method, as the amount of NaOH formed as a secondary product during the formation of BaSO$_4$ might not be sufficient for the complete dissolution of the BFS required for producing the solid composite.

In method B, on the other hand, the formation of BaSO$_4$ occurs in parallel with the dissolution of BFS and the consequent formation of reaction products derived from the alkali-activation reaction. This means that Ba(OH)$_2$ plays a double role in these systems: it is acting as activator to promote the hardening of the slag, and as a precursor reacting with Na$_2$SO$_4$ to

form $BaSO_4$. No traces of unreacted Na_2SO_4 in this system suggests the largely complete conversion of sulphate ions to $BaSO_4$ in the composition range assessed.

5. Conclusions

These results reveal that the immobilisation of soluble sulphate-bearing aqueous wastes is effectively achievable in $Ba(OH)_2$-BFS composites via either a one-step or two-step process, promoting the simultaneous formation of $BaSO_4$ and the activation of the BFS, favouring the formation of a stable cement-like composite. The order of mixing of $Ba(OH)_2$ in the system has a strong effect on the phase development of the cement wasteforms. A two-step process favours the formation of hydrotalcite and C-S-H, typically identified as main reaction products in NaOH-activated BFS binders. In the one step process crystalline hydrotalcite is not identified, and instead ettringite, barium carbonate and portlandite are formed. The direct inclusion of $Ba(OH)_2$ with the BFS and sulphate seems to provide extra alkalinity to the system, favouring an extended reaction of the BFS, and more formation of C-S-H products, along with the formation of $BaSO_4$.

This study has demonstrated that $Ba(OH)_2$-BFS composites represent an attractive and feasible alternative for surpassing the challenges associated with the immobilisation of sulphate aqueous wastes in the nuclear industry.

Acknowledgements

References

1. I. Sobolev, S. Dmitriev, F. Lifanov, A. Kobelev, S. Stefanovsky, and M. Ojovan: 'Vitrification processes for low, intermediate radioactive and mixed wastes', Glass Technol. Eur. J. Glass Sci. Technol. A, 2005, **46**, 28-35.
2. J. Sharp, J. Hill, N. Milestone, and E. Miller: 'Cementitious systems for encapsulation of intermediate level waste', Proceedings 9th International Conference on Radioactive Waste Management and Environmental Remediation, 2003, 21-25.

3. P.A. Bingham, N.C. Hyatt, R.J. Hand, and C.R. Wilding, "Glass development for vitrification of Wet Intermediate Level waste from Decomissioning of the Hinkley Point 'A' site." Mater. Res. Soc. Symp. Proc. 2009, **1124**, 161-166.

4. P. Bingham and R. Hand: 'Sulphate incorporation and glass formation in phosphate systems for nuclear and toxic waste immobilization', Mater Res Bull, 2008, **43**, 1679-1693.

5. R.S. Gollop and H.F.W. Taylor: 'Microstructural and microanalytical studies of sulfate attack. IV. Reactions of a slag cement paste with sodium and magnesium sulfate solutions', Cem. Concr. Res., 1996, **26**, 1013-1028.

6. H.F.W. Taylor, C. Famy, and K.L. Scrivener: 'Delayed ettringite formation', Cem. Concr. Res. , 2001, **31**, 683-693.

7. F.P. Glasser: 'Progress in the immobilization of radioactive wastes in cement', Cem. Concr. Res., 1992, **22**, 201-216.

8. X. Wu, S. Yen, X. Shen, M. Tang, and L. Yang: 'Alkali-activated slag cement based radioactive waste forms', Cem. Concr. Res., 1991, **21**, 16-20.

9. C. Shi and A. Fernández-Jiménez: 'Stabilization/solidification of hazardous and radioactive wastes with alkali-activated cements', J. Hazard. Mater., 2006, **B137**, 1656-1663.

10. N.B. Milestone: 'Reactions in cement encapsulated nuclear wastes: Need for toolbox of different cement types', Adv. Appl. Ceram., 2006, **105**, 13-20.

11. Y. Bai, N. Collier, N. Milestone, and C. Yang: 'The potential for using slags activated with near neutral salts as immobilisation matrices for nuclear wastes containing reactive metals', J. Nucl. Mater., 2011, **413**, 183-192.

12. A. Ipatti: 'Solidification of ion-exchange resins with alkali-activated blast-furnace slag', Cem. Concr. Res., 1992, **22**, 281-286.

13. T. Hanzlíček, M. Steinerova, and P. Straka: 'Radioactive metal isotopes stabilized in a geopolymer matrix: Determination of a leaching extract by a radiotracer method', J. Am. Ceram. Soc., 2006, **89**, 3541-3543.

14. E.M. Pierce, K.J. Cantrell, J.H. Westsik, K.E. Parker, W. Um, M.M. Valenta, and R.J. Serne: 'Report PNNL-19505: Secondary waste form screening test results - Cast stone and alkali alumino-silicate geopolymer', Pacific Northwest National Laboratory, 2010.

15. W. Gong, W. Lutze, and I.L. Pegg: 'Low-temperature solidification of radioactive and hazardous wastes', Patent, 2010.

16. T. Asano, T. Kawasaki, N. Higuchi, and Y. Horikawa: 'Feasibility study of solidification for low-level liquid waste generated by sulfuric acid elution treatment of spent ion exchange resin', J. Power Energy Syst., 2008, **2**, 206-214.

17. Y. Esen and B. Yilmazer: 'An investigation of X-ray and radio isotope energy absorption of heavyweight concretes containing barite', Bull Mater Sci, 2011, **34**, 169-175.

18. M. Ben Haha, G. Le Saout, F. Winnefeld, and B. Lothenbach: 'Influence of activator type on hydration kinetics, hydrate assemblage and microstructural development of alkali activated blast-furnace slags', Cem. Concr. Res., 2011, **41**, 301-310.

19. L. Alarcon-Ruíz, G. Platret, E. Massieu, and A. Ehrlacher: 'The use of thermal analysis in assessing the effect of temperature on a cement paste. ', Cem Concr Res, 2005, **35**, 609-613.

20. C. Hall, P. Barnes, A.D. Billimore, A.C. Jupe, and X. Turrillas: 'Thermal decomposition of ettringite $Ca_6[Al(OH)_6]_2(SO_4)_3.26H_2O$', J. Chem Soc. Faraday. Trans., 1996, **92**, 2125-2129.

21. M. Maciejewski, H.-R. Oswald, and A. Reller: 'Thermal transformations of vaterite and calcite', Thermochim Acta, 1994, **234**, 315-328.

22. F. Rey and V. Fornes: 'Thermal decomposition of hydrotalcites', J. Chem. Soc. Faraday Trans., 1992, **88**, 2233-2238.

23. H. Gaus and W. Lutze: 'Kinetics of strontium/barium and strontium/calcium ion exchange in synthetic zeolite A', J. Phys. Chem., 1981, **85**, 79-84.

24. S. Bernal, J. Skibsted, and D. Herfort: 'Hybrid binders based on alkali sulfate-activated Portland clinker and metakaolin', XIII International Congress on the Chemistry of Cement, Madrid, 3-8 July 2011, 2011, CD-ROM proceedings.